11-12-2015

Preparation and Evaluation of Phospholipid-Based Complex of Standardized Centella Extract (SCE) for the Enhanced Delivery of Phytoconstituents

Suprit Saoji
R.T.M. Nagpur University

Nishikant Raut
R.T.M. Nagpur University

Pradip Dhore
R.T.M. Nagpur University

Chandrashekhar D. Borkar
R.T.M. Nagpur University

Michael Popielarczyk
St. John Fisher College, mpp03870@students.sjfc.edu

Publication Information

Saoji, Suprit; Raut, Nishikant; Dhore, Pradip; Borkar, Chandrashekhar D.; Popielarczyk, Michael; and Dave, Vivek S. (2015). "Preparation and Evaluation of Phospholipid-Based Complex of Standardized Centella Extract (SCE) for the Enhanced Delivery of Phytoconstituents." *The AAPS Journal* 18.1, 102-114.
Please note that the Publication Information provides general citation information and may not be appropriate for your discipline. To receive help in creating a citation based on your discipline, please visit http://libguides.sjfc.edu/citations.

Preparation and Evaluation of Phospholipid-Based Complex of Standardized Centella Extract (SCE) for the Enhanced Delivery of Phytoconstituents

Abstract

In the present study, a phospholipid-based complex of standardized *Centella* extract (SCE) was developed with a goal of improving the bioavailability of its phytoconstituents. The SCE-phospholipid complex was prepared by solvent evaporation method and characterized for its physicochemical and functional properties. Fourier transform infrared spectroscopy (FTIR), differential scanning calorimetry (DSC), scanning electron microscopy (SEM), photomicroscopy, and powder x-ray diffraction (PXRD) were used to confirm the formation of *Centella* naturosome (CN). The prepared complex was functionally evaluated by apparent solubility, *in vitro* drug release, *ex vivo* permeation, and *in vivo* efficacy studies. The prepared CN exhibited a significantly higher (12-fold) aqueous solubility (98.0 ± 1.4 μg/mL), compared to the pure SCE (8.12 ± 0.44 μg/mL), or the physical mixture of SCE and the phospholipid (13.6 ± 0.4 μg/mL). The *in vitro* dissolution studies revealed a significantly higher efficiency of CN in releasing the SCE (99.2 ± 4.7, % *w*/*w*) in comparison to the pure SCE (39.2 ± 2.3, % *w*/*w*), or the physical mixture (42.8 ± 2.09, % *w*/*w*). The *ex vivo* permeation studies with the *everted intestine* method showed that the prepared CN significantly improved the permeation of SCE (82.8 ± 3.7, % *w*/*w*), compared to the pure SCE (26.8 ± 2.4, % *w*/*w*), or the physical mixture (33.0 ± 2.7, % *w*/*w*). The *in vivo* efficacy studies using the Morris Water Maze test indicated a significant improvement of the spatial learning and memory in aged mice treated with CN. Thus, drug-phospholipid complexation appears to be a promising strategy to improve the aqueous solubility and bioavailability of bioactive phytoconstituents.

Disciplines

Pharmacy and Pharmaceutical Sciences

Comments

This is the accepted manuscript of the article. The final article was published as: Saoji, S.D., Raut, N.A., Dhore, P.W. et al. Preparation and Evaluation of Phospholipid-Based Complex of Standardized Centella Extract (SCE) for the Enhanced Delivery of Phytoconstituents. *AAPS J* (2016) 18: 102. https://doi.org/10.1208/s12248-015-9837-2

Authors

Suprit Saoji, Nishikant Raut, Pradip Dhore, Chandrashekhar D. Borkar, Michael Popielarczyk, and Vivek S. Dave

Preparation and evaluation of phospholipid-based complex of Standardized Centella Extract (SCE) for the enhanced delivery of phytoconstituents.

Suprit D. Saoji[1*], Nishikant A. Raut[1*], Pradip W. Dhore[1], Chandrasekhar D. Borkar[1], Michael Popielarczyk[2], Vivek S. Dave[2**]

[1]Department of Pharmaceutical Sciences, R.T.M. Nagpur University, Nagpur, India

[2]St. John Fisher College, Wegmans School of Pharmacy, Rochester, New York, USA

*equal contribution

***Corresponding author*

Assistant Professor (Department of Pharmaceutical Sciences)

St. John Fisher College, Wegmans School of Pharmacy,

Rochester, NY, 14534

E-mail: viveksdave@gmail.com

Ph: 1-443-789-8649

Running Title:

Preparation and evaluation of phospholipid-based naturosomes of Standardized Centella Extract (SCE) for the enhanced delivery of phytoconstituents

Abstract

In the present study, a phospholipid-based complex of Standardized Centella Extract (SCE) was developed with a goal of improving the bioavailability of its phytoconstituents. The SCE-phospholipid complex was prepared by solvent evaporation method, and characterized for its physicochemical and functional properties. Fourier transform infrared spectroscopy (FTIR), differential scanning calorimetry (DSC), scanning electron microscopy (SEM), photomicroscopy, and powder x-ray diffraction (PXRD) were used to confirm the formation of CN (Centella Naturosome). The prepared complex was functionally evaluated by apparent solubility, *in-vitro* drug release, *ex-vivo* permeation, and *in-vivo* efficacy studies. The prepared CN exhibited a significantly higher (12-fold) aqueous solubility (98.01 ± 1.37 µg/mL), compared to the pure SCE (8.12 ± 0.44 µg/mL), or the physical mixture of SCE and the phospholipid (13.58 ± 0.35 µg/mL). The *in-vitro* dissolution studies revealed a significantly higher efficiency of CN in releasing the SCE (99.23 ± 4.71, % w/w) in comparison to the pure SCE (39.21 ± 2.31, % w/w), or the physical mixture (42.8 ± 2.09, % w/w). The *ex-vivo* permeation studies with the *everted intestine* method showed that the prepared CN significantly improved the permeation of SCE (82.83 ± 3.73, % w/w), compared to the pure SCE (26.84 ±2.41, % w/w), or the physical mixture (32.99 ±2.7, % w/w). The *in-vivo* efficacy studies using *Morris Water Maze* test indicated a significant improvement of the spatial learning and memory in aged mice treated with CN. Thus, drug-phospholipid complexation appears to be a promising strategy to improve the aqueous solubility and bioavailability of bioactive phytoconstituents.

Introduction

The use of natural products in the management of several diseases/disorders have gained popularity in recent years. However, their use as pharmaceutical drug products is limited due to the poor oral bioavailability of bioactive phytoconstituents. The poor bioavailability of these pharmacologically active components is mainly attributed to the high molecular weight/size, poor aqueous/lipid solubility, and lower plasma membrane permeability, thereby limiting their use for the effective treatment of various diseases and disorders (1, 2).

Improving the bioavailability of these bioactive compounds via improving the solubility and the permeability remains a major bottleneck in the development of pharmaceutical drug products from these entities. Among the several approaches explored in recent years for the improvement of bioavailability of drugs, drug-phospholipid complexes appear to be among the promising ones. Incorporating bioactive phytoconstituents into phospholipid molecules is reported to improve the aqueous solubility, the membrane permeability, and hence the systemic absorption and bioavailability of the active phytoconstituents. Such complexes are appropriately called *Phytosomes*, *Herbosomes*, or *Naturosomes* (3, 4). Studies have reported success in improving the pharmacological profiles of several bioactive phytoconstituents using drug-phospholipid complexation technique (5-9).

Alzheimer's disease (AD) is an irreversible, neurodegenerative disorder resulting in a progressive decline of cognitive and functional abilities, with impairment of memory and thinking skills (10). Alzheimer's Association projects the incidence of AD to 1 million people annually, and estimates the total prevalence of the disorder to 11-16 million people, by the year 2050 (11). Current AD interventions include symptomatic treatment with cholinesterase inhibitors (ChEIs) such as donepezil, and N-methyl-D-aspartase receptor antagonists such as memantine (12). However, the progression of the disease, and the associated neuronal degeneration continues, in addition to the adverse effects of this treatment (13). In 2004, the USFDA approved Galantamine, a phytoconstituent obtained from Galanthus *nivalis*, for the treatment of AD with the reported mechanism being the inhibition of acetyl cholinesterase (14). Recently, some herbal extracts such as those of Ginkgo *biloba*, and other phytochemicals such as evodamine have also been explored for their anti-AD properties in animals and humans (15-19).

Centella asiatica Linn. (Apiaceae), a perennial creeper found throughout most tropical and subtropical countries, is reported to be useful for anxiety, memory enhancement, and

neuroprotection (20). The major chemical constituents reported to be responsible for its pharmacological activity are triterpenes based on steroidal moieties, such as asiaticoside, asiatic acid, madecassoside, and madecassic acid (21). Several pharmaceutical products containing C. asiatica are commercially available, and are recommended for enhancing memory in patients with memory deficit (22). The usefulness of any pharmaceutical product depends on the safety, efficacy, and the quality of that product. A Quality by Design (QbD) approach is now considered to be an ideal pathway to ensure the development of a quality product, and the minimization of product variabilities. QbD is broadly defined as a scientific, risk-based, holistic, and a proactive approach to pharmaceutical development that begins with predefined objectives, and emphasizes the understanding and control of the product and processes based on sound science, and quality risk management (23). Despite the commercial availability of several pharmaceutical products containing extracts of Centella asiatica, the issue of the low aqueous solubility of the extract remains practically unaddressed.

Thus, the primary goal of the current study was to evaluate the feasibility of enhancing the aqueous solubility of Standardized Centella Extract (SCE) by preparing its vesicular complex with hydrogenated soy phosphatidylcholine (Phospholipon® 90H). This complex is hereby referred to as Centella Naturosome (CN). To address this objective, CN were prepared using a solvent evaporation method. The formulation and the process variables for the preparation of the CN were optimized using a QbD approach. Response surface analysis by the means of central composite design was employed for the optimization of the critical process parameters (CPP) on the SCE entrapment rate of CN. The prepared CN were evaluated for their physicochemical, functional, and preliminary pharmacological properties.

Materials and methods

Materials

The Standardized Centella Extract (SCE), containing ~30% triterpenes was obtained from Natural Remedies Ltd, Bangalore, India. The identity of the SCE was confirmed by HPLC analysis. Hydrogenated soy phosphatidylcholine (Phospholipon® 90H) was generously gifted by Lipoid, Ludwigshafen, Germany. All other chemicals and reagents used were of analytical grade.

Analysis of the triterpenes present in SCE

The concentrations of the triterpenes present in SCE i.e. asiaticoside, asiatic acid, madecassoside, and madecassic acid, were determined using a modified, reverse-phase high performance – liquid

chromatography (RP-HPLC) method previously described by Hashim et al. (21). Briefly, the HPLC system (Model: Prominence, Shimadzu Corporation, Kyoto, Japan) with LC solution software, equipped with a LC-20AD HPLC pump, a manual rheodyne sample injector, and a SPD-M20A detector were used. The mobile phase was composed of acetonitrile and water (25:75, v/v), at a flow rate of 1.5 mL/min. A Micra- NPS RP18 column (33×8.0×4.6 mm, 1.5 μm) was used as a stationary phase, and the detector wavelength was 210 nm at room temperature. Throughout the study, the suitability of the chromatographic system was monitored by calculating the trailing/asymmetry factor, theoretical plates and the relative standard deviation (RSD). The calibration curves for individual triterpenes were constructed by analyzing eight concentrations of the standard solution for each triterpene, and plotting peak areas versus concentration. The method was validated by analyzing the different validation characteristics such as linearity, accuracy and precision.

Preparation of Centella Naturosome (CN)

The CN were prepared by slightly modifying the solvent evaporation method described by Bhattacharyya et al. (24). Briefly, different ratios, i.e. 0.5:1, 1.01:1, 1.75:1, 2.49:1 or 3:1, of Phospholipon® 90H and SCE were placed in a 100 mL round bottom flask, and 40 mL of ethanol was added to the mixture. The reaction was controlled and maintained at various temperatures, i.e. 40°C, 44°C, 50°C, 56°C, or 60°C using a water bath. The reaction was carried out for different durations, i.e. 1h, 1.4h, 2h, 2.6h or 3 h. The resulting clear solution was evaporated to 2–3 mL, and an excess of n-hexane was added to it with continuous stirring. The dispersion formed was then precipitated, filtered, and dried under vacuum to remove any traces of solvents. The resulting CN were stored at room temperature, in amber colored glass vials, flushed with nitrogen, for further testing.

Quality by Design (QbD) based design of experiments

A QbD-based approach using a central composite design to obtain a response surface design was employed to systematically study the combined influence of the formulation and process variables such as the phospholipid-to-drug ratio (X_1, w:w), the reaction temperature (X_2, ˚C), and the reaction time (X_3, h) on the Critical Quality Attributes (CQAs) of the product i.e. the entrapment efficiency. Using this design, the influence of three factors was evaluated, and the experimental trials were carried out at all 20 possible combinations (25, 26). A statistical model incorporating interactive and polynomial terms was used to evaluate the response employing the following equation (1):

$$Y = b_0 + b_1X_1 + b_2X_2 + b_3X_3 + b_{11}X_1^2 + b_{22}X_2^2 + b_{33}X_3^2 + b_{12}X_1X_2 + b_{23}X_2X_3 + b_{13}X_1X_3 \quad (1)$$

Where, Y was the dependent variable, b_0 is the arithmetic mean response of the 20 runs, and b_i is the estimated coefficient for the factor X_i. The main effects (X_1 and X_2) represented the average result of changing one factor at a time from its low to high value. The interaction terms (X_1X_2, X_2X_3, X_1X_3) showed how the response changes when all three factors were simultaneously changed. The polynomial terms (X_1^2, X_2^2, and X_3^2) were included to investigate on-linearity. The level values of the three factors, the real values of the central composite design batches, and the resulting entrapment efficiencies are shown in table 1 and 2.

Entrapment efficiency of CN

The entrapment efficiency, i.e. the SCE (total triterpenes content) entrapped in the naturosome was determined using a combination of methods described in the literature (27, 28). Briefly, accurately weighed (100 mg) CN powder was dispersed in 10 mL chloroform. The CN and Phospholipon® 90H both were easily dissolved in the chloroform. The SCE not entrapped in the CN was collected as a sediment and assayed by HPLC. The entrapment efficiency of the prepared CN was calculated using the following equation (2):

$$Entrapment\ efficiency\ (\%) = \frac{C_t - C_f}{C_t} \times 100 \qquad (2)$$

Where, C_t = Total concentration of SCE, and C_f = SCE contained in the filtrate.

Determination of SCE content in CN

The SCE content in the CN was determined by HPLC method described above. The drug content was calculated using equation (3) below, previously described by Bhattacharya et al.(29).

$$Drug\ content\ (\%) = \frac{Amount\ of\ drug\ in\ CN}{Amount\ of\ CN} \times 100 \qquad (3)$$

Physico-chemical characterization of CN

Photomicroscopy

For the microscopic characterization of the prepared naturosomes, a suspension containing approximately 100 mg of the naturosome powder was transferred to a glass tube and diluted with 10 mL Phosphate Buffer Saline (PBS, pH 7.4). The suspended vesicles were then mounted on a clear glass slide and photomicrographs were captured with a microscope (Model: DM 2500, Leica Microsystems, Germany) under 20x magnification.

Scanning Electron Microscopy (SEM)

The CN powder obtained from the optimized formulation batches was sprinkled on a double-sided carbon tape, and the tape was placed on a brass stub. The surface powder was coated with a thin layer of palladium using the auto fine coater (Model: JFC1600, Jeol Ltd., Tokya, Japan). The palladium coated samples were observed using a Scanning Electron Microscope (Model: JSM-6390LV, Jeol Ltd, Tokyo, Japan) equipped with a digital camera, at 10 KV accelerating voltage.

Particle size and zeta potential analysis

The particle size analysis of the prepared CN was carried out using Photon Correlation Spectroscopy (PCS), with dynamic light scattering on a Zetasizer® nano (Model: Zen 3600, Malvern Instruments, Malvern, UK) equipped with a 5mW He-Ne laser with a wavelength output of 633 nm. The measurements were carried out at 25 °C, at an angle of 90° and a run time of at least 40-80 sec. Water was used as a dispersant. The zeta potential was measured by Smoluchowski's equation from the electrophoretic mobility of naturosomes (30). All measurements were performed in triplicate.

Fourier Transform Infrared (FTIR) Spectroscopy

The infrared spectra of neat SCE, Phospholipon® 90H, the physical mixture of SCE with Phospholipon® 90H (PM), and the prepared CN were obtained from an FTIR spectrophotometer (Model: IR Prestige-21, Shimadzu, Japan) equipped with an Attenuated Total Reflectance (ATR) accessory. The analysis of the samples was carried out using diffuse reflectance spectroscopy using KBr compacts. The influence of the residual moisture was theoretically removed by subjecting the samples to vacuum drying before obtaining any spectra. Each sample analysis included 45 scans, at a resolution of 4 cm^{-1} in the wavelength range 4000 to 600 cm^{-1}.

Differential scanning calorimetry (DSC)

The thermal analysis of the samples (SCE, Phospholipon® 90H, PM, and CN) was carried out using a differential scanning calorimeter (Model: Q20, TA Instruments, Inc., New Castle, DE, USA). The analysis was performed under a purge of dry nitrogen gas (50 ml/min). High-purity indium was used to calibrate the heat flow and the heat capacity of the instrument. The samples (~5 mg) were held in open standard aluminum pans. Each sample was subjected to a single heating cycle from 0°C to 400°C at a heating rate of 10°C/min. The peak transition onset temperatures of samples were analyzed using the Universal Analysis software version 4.5A, build 4.5.0.5 (TA Instruments, Inc., New Castle, DE, USA) (31).

Powder x-ray diffraction (PXRD)

The polymorphic state of the samples (SCE, Phospholipon® 90H, PM, and CN) was evaluated using a powder x-ray diffractometer (Model: D2 Phaser, Bruker AXS, Inc., Madison, WI, USA), equipped with a Bragg-Brentano geometry (θ/2θ) optical setup. The samples were scanned with the diffraction angle increasing from 2º to 90º, 2θ angle, with a step-angle of 0.2º 2θ and a count time of 0.5 seconds.

Functional evaluation of CN

Apparent solubility analysis

The apparent solubility of the samples was determined by a method previously described by Singh et al. (32). Briefly, an excess of SCE and CN were added to 10 mL of water or n-Octanol in sealed glass containers at room temperature (25°C). The liquid was agitated for 24 h, followed by centrifugation for 30 min at 4,000 RPM. The supernatant was filtered through a membrane filter (0.45 µ). 1 mL of this filtrate was mixed with mobile phase to prepare appropriate dilutions, and the samples were analyzed at 210 nm using the RP-HPLC method described above.

In-vitro drug release (dissolution)

The *in-vitro* dissolution study was carried out using the method described previously by Zhang et al (33). Accurately weighed samples equivalent to 50 mg of SCE were added to the surface of the stirred dissolution medium (900 mL phosphate buffer, pH 6.8) at the beginning of the study in a USP type II dissolution apparatus (Model: TDT-06T, Electrolab India Pvt. Ltd., India). The dissolution was carried out at 100 rpm and 37ºC. Samples (10 mL) from the dissolution medium were withdrawn at regular time intervals, and replaced with an equal volume of fresh medium to maintain sink conditions. The samples were filtered through a membrane filter (0.45µ), diluted suitably with mobile phase to prepare dilutions, and analyzed using the RP-HPLC method described above.

Dissolution efficiency (DE)

The dissolution efficiency (DE) of the SCE, PM, and CN in the phosphate buffer saline was evaluated at 12 h. The dissolution efficiency was calculated using the equation (4) below, previously described by Anderson et al. (34).

$$DE = \frac{\int_{t_1}^{t_2} y.dt}{y_{100} \times (t_2 - t_1)} \times 100 \qquad (4)$$

Where, y is the percentage of dissolved drug. DE is the area under the dissolution curve between time points t_1 and t_2 expressed as a percentage of the curve at maximum dissolution, y_{100}, over

187 the same time period. The integral of the numerator, i.e. the area under the curve was calculated
188 by a model independent trapezoidal method as defined by the equation (5) below.

189 $$AUC = \sum_{i=1}^{i=n} \frac{(t_1 - t_{i-1})(y_{i-1} + y_i)}{2} \qquad (5)$$

190 Where t_i is the i^{th} time point, y_i is the percentage of dissolved drug at time t_i.

191 ***Ex-vivo permeability***

192 *Perfusion apparatus*: The apparatus used in this study was previously described by Dixit et al.
193 (35) which consisted of a two glass tubes held together by a glass joint on the upper end with
194 open tapering ends facing towards each other. A provision for mounting the tissue is facilitated
195 in the form of a bulge at the ends of both tubes. The dimensions of the apparatus (18cm × 4cm ×
196 2cm) are such that it can be conveniently set up in a 250 mL glass measuring cylinder. After
197 mounting the everted intestinal segment on the apparatus the whole assembly is kept in a glass
198 measuring cylinder; the inside of the glass tubes serve as the receiver compartment and the
199 outside serves as the donor compartment.

200 *Isolation and eversion of the intestine*: Ethical clearance for the handling of experimental
201 animals was obtained from the institutional animal ethics committee (IAEC) formed for this
202 purpose. The Sprague-Dawley® rats (200-250 g) were fasted overnight. The rat was euthanized
203 humanely by cervical dislocation, midline incision was given to open the abdomen and the
204 intestine was carefully maneuvered to identify the ileo-cecal junction. About 7cm long intestine
205 (jejunum) was removed from the mesenteric attachments carefully without damaging the
206 intestine. The isolated piece of intestine was thoroughly washed with Kreb's solution, everted
207 using glass rod, and transferred to a petri dish containing Kreb's solution. A 6cm everted segment
208 was used for permeability experiments.

209 *Permeability determination*: The everted piece of intestine was mounted between the two tapered
210 ends of the perfusion apparatus. The perfusion apparatus was filled with Kreb's solution and
211 immersed in the measuring cylinder (250 mL) containing SCE, PM, or CN (100 µg/mL) in 250
212 mL Kreb's solution. The whole assembly was placed on a constant temperature (37 °C) magnetic
213 stirrer and the content stirred at 25 RPM. Additionally, the Kreb's solution was constantly
214 aerated with carbogen (Oxygen: Carbon dioxide (95:5) mixture). The samples were collected at
215 15 min interval up to three hours and analyzed by HPLC for estimation of permeability.

Preliminary pharmacological evaluation (*in-vivo* efficacy)

Animals: Young (3-4 months), and aged (22-24 months), male Swiss albino mice were group housed under constant room temperature (25 ± 2 °C), relative humidity (50 - 70% RH), and maintained on a 12 hour: 12 hour light: dark cycle. Food and water were given *ad libitum* except during the experiment. All procedures and protocols employed in the study were approved and carried out under strict compliance with the Institutional Animal Ethics Committee, Department of Pharmaceutical Sciences, R. T. M. Nagpur University, Nagpur, MS, India.

Morris Water Maze Test (MWM): The MWM test was performed to compare the pharmacological efficacy of the prepared CN with that of SCE in spatial learning and memory in mice. MWM test is among the most widely used behavioral models employed for screening of anti-Alzheimer's activity in the rodents. The standard protocol previously described by Vorhees et al. was employed with some modifications (36). Briefly, the animals were acclimatized to the laboratory conditions for a week before performing the actual experiments. MWM consists of a large circular pool measuring 90 cm in diameter and 40 cm in height. The maze was filled with water (25 °C) to a height of 30 cm, and rendered opaque using milk. The pool was arbitrarily divided into four compass quadrants, and a white escape platform (10 cm in diameter) was submerged in one of the quadrants, one cm below the water surface. The location of platform remained fixed for all four days of training sessions.

The animals were divided into **seven** groups with six animals in each group (n=6), i.e. **group 1: young mice (vehicle), group 2: aged mice (vehicle), group 3: Phospholipon® 90H (900 mg/kg), group 4: piracetam (200 mg/kg), group 5: SCE (300 mg/kg), group 6: PM (equivalent to 300 mg/kg SCE),and group 7: CN (equivalent to 300 mg/kg SCE).** The doses used in the present study were reported effective in the animals (37, 38). All animals received their respective treatments orally, each day, one hour before the experiment. Each mouse was given four training sessions per day, at an interval of 10 minutes between the training sessions, for four consecutive days. The starting locations for the animals varied quasi-randomly, and the cutoff time was fixed at 120 seconds. The length of time taken by the animal to locate the platform was measured as escape latency. If the animal failed to escape within 120 seconds, it was manually placed on the platform for 30 seconds, and the escape latency was recorded as 120 seconds. A single 120 second probe trial was also conducted on the 5th day (24 hours after the

last acquisition trial), to measure the time spent in the target quadrant, as a measure of memory retention.

Results and discussion

Preparation of Centella Naturosome (CN)

The initial investigation of the influence of factors revealed that all the studied factors, i.e. the phospholipid-to-drug ratio, the reaction temperature, and the reaction time had a significant influence on the entrapment efficiency of the prepared naturosomes. The results of the entrapment efficiency (%) are shown in Table 2. The measured values from the experimental trials revealed a wide range (58.1– 95.1, % w/w) entrapment efficiencies (Table 2). The fitted polynomial equations relating the response (entrapment efficiency, % w/w) to the transformed factors are shown in Figure 1. The polynomial equations could be used to draw conclusions after considering the magnitude of the coefficient, and its associated mathematical sign, i.e., positive or negative. The results from the Figure 1 also indicated that all the coefficients, i.e. b_1, b_2, b_3, b_{11}, b_{22}, b_{33}, b_{12}, b_{23}, and b_{13} were statistically significant ($p < 0.05$). The value of correlation coefficient (R^2) was found to be 0.9369, indicating a good fit to the quadratic model. The multiple regression analysis (Figure 1) revealed that the coefficients b_1, b_2, and b_3 were positive. This indicated that the entrapment efficiency increased with increasing X_1, X_2, and X_3. **The data further indicated that the quadratic model is statistically significant ($F_{critical}$ value = 16.5; p <0.001) (Suppl. Table 1)**.

Based on the central composite design, the response surface and contour plots depicting the changes in the entrapment efficiency (%) as a function of X_1, X_2, and X_3 were created (Suppl. Figure 1). The data from all 20 batches of the central composite design were used for generating interpolated values using Design Expert 9, version 9.0.4.1 (Stat-Ease, Inc., Minneapolis, MN). The response surface and contour plots indicated a strong influence of the studied factors X_1, X_2, and X_3 on the entrapment efficiency. Increasing levels of X_1, X_2, and X_3 were found to be favorable conditions for obtaining higher entrapment efficiency. Based on these observations, along with the multiple regression model, the optimal values of the studied factors, i.e. the phospholipid-to-drug ratio, the reaction temperature, and the reaction time were 3:1, 60 °C, and 3 hours, respectively.

Validation of the model

In order to validate the developed model, an additional batch of CN was prepared. This validation batch was prepared using the optimal settings of the formulation and process variables from the model, i.e. X_1, X_2, and X_3 values of 3:1, 60 °C, and 3 hours, respectively. The predicted entrapment efficiency of the CN obtained from model, as well as the actual entrapment efficiency achieved from the prepared formulation were compared **(Suppl. Table 2)**. The average entrapment efficiency of SCE in naturosomes prepared under the optimized conditions was found to be 93.9 ± 1.3 %. These values compared well with the model-predicted value, i.e. 95.0 %, indicating the practicability, and the validity of the developed model. The bias (%), calculated using the equation (6) below was also found to be less than 3% (1.2%), indicating the relative robustness of the model (39).

$$Bias\ (\%) = \frac{predicted\ value - observed\ value}{predicted\ value} \times 100 \qquad (6)$$

Physico-chemical characterization of the prepared CN

Photomicroscopy and Scanning electron microscopy (SEM)

The results from the initial morphological characterization of SCE and the prepared CN showed that the SCE appeared to be irregularly shaped, polydispersive agglomerates made up of small, crystalline particles (Suppl. Figure 2A). Whereas, the prepared CN appeared to have a dramatically different morphology (Suppl. Figure 2B). These particles were much larger entities, with a relatively rough surface; and appeared to consist of multiple layers, with possibly entrapping the SCE crystals (shown by the red pointer).

The prepared CN were further analyzed by SEM for their surface morphology [Suppl. Figure 3 (A, B, and C)]. The electron micrographs at different magnifications i.e. 1000x (3A), 3000x (3B), and 6000x (3C) revealed the formation of multi-layered vesicles of hydrogenated soy phosphatidylcholine. The initial morphological characterization indicated the successful formulation of phospholipid-based vesicular complex (naturosome) of SCE.

Particle size and zeta potential analysis

The mean particle size and the zeta potential values of the prepared CN were carried out using dynamic light scattering technique [Suppl. Figure 4(A andB)]. The mean particle size of CN was found to be 450.1 ± 20.0 nm. The surface area/volume (SA/V) ratio of most particles is inversely proportional to the particle size. Thus, smaller particles of the CN, having a higher SA/V, makes it easier for the entrapped drug to be released from the naturosome via diffusion

and surface erosion. They also have the added advantage for the drug-entrapped naturosomes to penetrate into, and permeate through the physiological drug barriers. LeFevre et al. and Savic et al. have previously suggested that larger particles (≤ 5 mm) are taken up via the lymphatics, while the smaller particles (≤ 500 nm) can cross the epithelial cell membrane via endocytosis (40, 41). Zeta potential is another important index commonly used to assess the stability of the naturosomes. The zeta potential of the prepared CN was found to be -35.0 ± 1.9 mV. These results are in agreement with previous reports, which mentions that the zeta potential values of greater than −30 mV are considered acceptable, and are indicative of a good physical stability (42, 43).

Fourier transform infrared Spectroscopy (FTIR)

The results from the FTIR analyses of the SCE, Phospholipon® 90H, the physical mixture of SCE with Phospholipon® 90H (PM), and the prepared CN are shown in Figure 2 (A, B, C, and D, respectively). The FTIR spectrum of SCE (Figure 6A) exhibited a broad peak at 3365 cm^{-1} representing the aliphatic alcoholic (–OH) group substituted on the cyclic ringed structure. The C-H stretching signal at 2926 cm^{-1} relates to the characteristic feature of the triterpene ring structure. The triterpene also exhibited a C=O stretching around 1710 cm^{-1}, along with a C=C stretching signal at 1662 cm^{-1} as an associated peak possibly representing the alkene nature of neighboring ring attachments. The FTIR spectrum of the SCE further exhibited the aromatic nature of the basic ring nucleus, with aromatic stretching signals in the region of 1602 cm^{-1} and 1563 cm^{-1}. Prominent peaks observed at 1164 cm^{-1} and 1088 cm^{-1} typically relates to the presence of acidic functional groups (-COOH) on the molecule.

The FTIR spectrum of Phospholipon® 90H revealed the characteristic C–H stretching signal present in the long fatty acid chain at 2,918 cm^{-1} and 2,850 cm^{-1} respectively. In addition, a C=O stretching band at 1,738 cm^{-1} in the fatty acid ester, a P=O stretching band at 1,236 cm^{-1}, a P–O–C stretching band at 1,091 cm^{-1}, and a $-N^{+}(CH_2)^3$ stretching at 970 cm^{-1} were also observed in the spectrum. In the FTIR spectrum of the prepared CN, the SCE peaks at 1602 cm^{-1} and 1662 cm^{-1} were found to have disappeared, with an emergence of a peak at 1635 cm^{-1} indicating a possibility of conjugation of the two compounds, leading to the formation of a naturosome. The disappearance of peak at 1563 cm^{-1} (exhibiting the aromatic ring stretching) may be due to the weakening, or removal, or shielding by the phospholipid molecule, which may further support the formation of naturosome. This phenomenon may be explained as occurring

due to the entrapment/packing of the SCE in the hydrophobic cavity of the formed phospholipid vesicle, and being held by van der Waals forces, and other hydrophobic interactions (44). The presence of the peaks at 1468 cm^{-1}, 1418 cm^{-1}, and 1378 cm^{-1} exhibits the C-H bending and rocking. These peaks were found in both Phospholipon® 90H, as well as in the physical mixture; and remained consistent in the complex with a negligible shift from original scale, indicating their lack of involvement in the formation of the naturosome.

Differential scanning calorimetry (DSC)

The interactions between multiple components of a formulation is commonly analyzed by DSC. Such interactions are typically observed as the elimination of endothermic peaks, appearance of new peaks, changes in peak shape and its onset, peak temperature/melting point and relative peak area, or enthalpy (45). The Figure 3 shows the DSC thermograms of (A) pure SCE, (B) Phospholipon® 90H, (C) PM, and (D) CN. The pure SCE (Figure 3A) revealed a broad endothermic peak around 94.4 ºC. Phospholipon® 90H showed two sharp endothermic peaks at 125.2 ºC and 182.5 ºC, respectively (Figure 3B). The first peak (at 125.2 ºC) is likely due to the melting of phospholipid. The second peak (at 182.5 ºC) appears to be due to the phase-transition from gel to a liquid-crystalline state, and the carbon-chain in the phospholipid may have perhaps undergone other isomeric or crystal changes (46). In the physical mixture (PM) of the SCE and Phospholipon® 90H (Figure 3C), the two peaks are observed at 100.9 ºC and at 123.6 ºC. It may be assumed that with the rise in temperature, the Phospholipon® 90H melts, and the SCE gets dissolved in it, partly forming the naturosome. The thermogram of the CN exhibits two partially fused, broad endothermic peaks at 68.8 ºC and 85.9 ºC, respectively (Figure 3D). These peaks differed from the peak of SCE and Phospholipon® 90H. A reduction in the melting point and enthalpy may account for the increased solubility, and reduced crystallinity of the drugs (47). It was thus evident that the original peaks of SCE and Phospholipon® 90H disappeared from the thermogram of the CN, and the phase transition temperature was lower than that of Phospholipon® 90H, thus confirming the formation of the drug-phospholipid complex. These findings are in agreement with those reported in the literature, and the interaction between the SCE and Phospholipon® 90H can be attributed to a combination of forces such as hydrogen bonding and van der Waals interactions, and can be considered as an indication of drug amorphization and/or complex formation, as supported by IR spectroscopy (48, 49). The interaction of the SCE with the polar region of Phospholipon® 90H may have been followed by

the entrapment of SCE with the long chain hydrocarbon tail of phospholipid molecules. This resulted in the sequential decrease in phospholipid hydrocarbon chains, and the disappearance of the second endothermic peak of Phospholipon® 90H with a reduction in the phase transition temperature (45).

Powder x-ray diffraction (PXRD)

The Figure 4 displays the powder x-ray diffraction patterns of (A) SCE, (B) Phospholipon® 90H, (C) PM, and (D) CN. The diffractogram of the SCE (Figure 4A) revealed sharp crystalline peaks at $2\theta = 46.0^{o}$, 41.0^{o}, 32.0^{o}, and 28.0^{o}. A single diffraction peak was observed at $2\theta = 21.0^{o}$ for Phospholipon® 90H (Figure 4B). The physical mixture (PM) showed most of the peaks associated with the SCE and Phospholipon® 90H (Figure 4C). In comparison to the physical mixture, the diffractogram of the CN revealed the disappearance of most of the crystalline peaks associated with the SCE (Figure 4D). These results were in agreement with the previously reported studies, where the disappearance of the Active Pharmaceutical Ingredient (API) peaks was associated with the formation of API-Phospholipid complexes (44, 48). The disappearance of the SCE crystalline peaks thus confirmed the formation of SCE-Phospholipid complex. It may then also be concluded that the SCE in the Phospholipon® 90H matrix may be present either as a molecularly dispersed, or an amorphous state (50).

Functional evaluation of CN

Apparent solubility

The results of the measured apparent solubilities of the pure SCE, the physical mixture of SCE and Phospholipon® 90H (PM), and the prepared SCE- Phospholipon® 90H complex (CN) are shown in the Table 3. It was observed that the pure SCE had poor aqueous solubility (~8 µg/mL), and a relatively higher solubility in n-Octanol (~325 µg/mL), indicating a rather lipophilic nature of the drug. The physical mixture (PM) revealed a non-significant change in the n-Octanol solubility, and a modest increase (~1.5 times) in the aqueous solubility. The prepared SCE- Phospholipon® 90H complex (CN) however, showed a dramatic, and a significant (over 12-fold) increase in the aqueous solubility. This increase in the solubility of the prepared complex may be explained by the partial amorphization (reduced molecular crystallinity) of the drug, and the overall amphiphilic nature of the naturosome (32, 51).

***In-vitro* drug release (dissolution)**

The results of in-vitro drug release studies are shown in the Figure 5. The 12 hours dissolution in the phosphate buffer (pH-6.8) revealed that, the pure SCE showed the slowest rate of dissolution,

i.e. at the end of the dissolution period only about 39% w/w of SCE was dissolved. The dissolution rate of the physical mixture was found not to be significantly different (~42% w/w dissolved in 12 hours) compared to the pure SCE. The prepared CN, however revealed a significantly faster release of SCE at the end of dissolution period. The dissolution profile of the CN followed a near zero-order release, and at the end of 12 hours, over 99% w/w SCE was observed to be released from the CN. The dissolution rate is largely influenced by the crystal morphology and the wettability of the solids, and the improved dissolution rate of SCE from the CN may be explained by the improved solubility, and the partially disrupted crystalline phase (amorphous form) in the prepared naturosome (5, 50). The relatively higher amorphous state of the naturosome, and their increased water-solubility may have had a positive impact on the cumulative release of the drug.

Dissolution efficiency (DE)

The dissolution efficiencies of the pure SCE, the physical mixture of SCE and Phospholipon® 90H (PM), and the prepared SCE- Phospholipon® 90H complex (CN) calculated from the *in-vitro* release studies in phosphate buffer (pH-6.8) were calculated using the equation 4 above (Suppl. Table 3). The prepared CN showed a significantly ($P<0.001$) improved dissolution efficiency compared to the pure SCE. Almost 2.4-fold increase in the DE was observed for CN in PBS at the end of 12 hours, compared to the pure SCE. This significant increase can be attributed to the enhancement of SCE solubility in the prepared naturosome. A marginal, but a statistically significant ($p < 0.01$) increase in dissolution efficiency of SCE in physical mixture, compared to the pure SCE was also observed. The solubilizing ability of the phospholipids, owing to their amphiphilic nature is likely the reason for this observed increase in the release of SCE.

***Ex-vivo* permeability**

The results of the ex-vivo permeability study as carried out with the *everted intestine* method on the pure SCE, the physical mixture of SCE and Phospholipon® 90H (PM), and the prepared SCE- Phospholipon® 90H complex (CN) are shown in the Figure 6. The permeability of the tested samples appeared to follow the trends observed in the *in-vitro* release study. It was observed that, at the end of three hour study duration, only about 26% w/w of the pure SCE permeated through the everted intestine. The physical mixture (PM) showed a marginal, but a non-significant improvement in the permeation of SCE. The prepared CN, however, demonstrated a significantly improved permeation of SCE across the everted intestine. At the

end of three hour testing period over 80 % w/w of SCE was found to permeate across the biological membrane. The phospholipids being amphiphilic in nature, may behave as surfactants and contribute towards the increased permeability of the drug across the membrane. Due to the observed improved solubility, increased dissolution rate, and observed increased permeability of the SCE in the prepared CN, this approach of the drug-phospholipid complexation lends itself to be a promising formulation strategy for the enhanced delivery of SCE to the physiology.

Preliminary pharmacological evaluation (*in-vivo* efficacy)

The results of the preliminary pharmacological evaluation (in-vivo efficacy) of the prepared SCE-Phospholipid complex (CN) are shown in the Figure 7. A group of young mice (n=6) was treated with the vehicle (saline). The aged mice (n=6/group) were administered with vehicle (saline), **Phospholipon® 90H (900 mg/kg),** piracetam (200 mg/kg), SCE (300 mg/kg), or CN (300 mg/kg SCE equivalent) via oral route. As shown in the Figure 7A. It was observed that the escape latency i.e. the time taken by the animal to locate the platform, in the young mice treated with vehicle progressively and significantly decreased during the five-day training period. This indicated a quicker learning and adaptation to the surroundings by these animals. The aged animals treated with the vehicle, however, exhibited a significantly higher escape latency **($p < 0.01$ on day 2, $p < 0.001$ on day 3 and 4),** that did not appear to significantly improve at the end of five-day training period. The aged animals treated with piracetam, SCE, or CN showed a significant decrease in the escape latency at the end of five-day training period. The application of two-way ANOVA showed the main effect of treatments [$F(4,100) = 26.02$, $p < 0.0001$], acquisition days [$F(3,100) = 81.45$, $p < 0.0001$], and their interaction [$F(12,100) = 2.906$, $p < 0.01$]. The post-hoc Bonferroni multiple comparison test also revealed that all the treatments (piracetam, $p < 0.001$ on day 3 and 4; SCE, $p < 0.05$ on day 3, and $p < 0.01$ on day 4, or CN, $p < 0.01$on day 2 and $p < 0.001$ on day 3 and 4) in aged animals significantly reduced escape latency on day two onward as compared to the vehicle treated aged animal group. While the CN and piracetam showed similar effects on the escape latency ($p > 0.05$), CN exhibited higher efficacy in terms of reduction in the escape latency as compared to the pure SCE ($p < 0.05$). **However, a four-day alone treatment with Phospholipon® 90H in aged mice did not reveal any significant improvements in the escape latency compared to the vehicle treated mice.**

In addition, the application of one-way ANOVA showed a significant effect of piracetam, SCE or CN treatments on time spent in the target quadrant [$F(4, 29) = 6.221$, $p < 0.01$] at the

end of five days (Figure 7B). The Bonferroni multiple comparison test revealed that aged animals treated with vehicle did not recognize the target quadrant, and therefore spent less time in that quadrant compared to the vehicle-treated young animals ($p < 0.05$). However, oral treatments of piracetam ($p < 0.01$), SCE ($p < 0.05$), or CN ($p < 0.01$) significantly increased the time spent in the target quadrant compared to the vehicle-treated aged animals**, thus confirming the potential effect of *centella extract* on memory as reported in earlier studies (37, 38). Centella extract is known to improve the morphology and arborization of hippocampal neuronal dendrites (52, 53). Moreover its negative effect on reactive oxygen species and superoxide formation along with decrease in glutathione, activation of glutathione-S-transferase, have reportedly the key mechanisms involved in its nootropic action (37).**

It was interesting to note here that, CN treatment showed a comparable effect to that of the standard piracetam treatment ($p > 0.05$) i.e., the CN treated animals spent more time in the target quadrant. The SCE treated mice, while showed an increased time spent in the target quadrant compared to the vehicle group, this effect was not statistically significant. Thus we suggest that although both, SCE or CN administration improves the spatial learning and memory in aged mice, CN exhibits better efficacy compared to SCE in MWM. The improvement in the relative absorption of CN after oral administration might be attributed to the following factors: SCE being lipophilic in nature, its absorption and bioavailability is dissolution rate limited. Interactions between the non-polar, fatty acid component of phospholipid and the SCE could have enhanced the overall hydrophilicity and solubility of CN (3). This may have possibly resulted in an improved dissolution efficiency of the CN. In addition, the smaller particle size of the prepared CN might have led to enhanced relative absorption of SCE after oral administration. The extended release of SCE from CN, along with a decreased metabolism may also confer a prolonged duration of action and higher bioavailability (28). Furthermore, as reported in the previous studies, the intestinal transport and the absorption mechanisms might also be the possible contributors to the improved CN oral bioavailability (54, 55).

Several studies have previously reported the influence of phospholipids on memory improvement (56-59). Since a phospholipid was employed in the present study as a carrier for the SCE in the formulation of the CN, we examined the possibility of the memory-enhancement effects of Phospholipon® 90H. The results from Phospholipon® 90H-treated

aged mice group showed no significant improvement in the escape latency or the time spent in the target quadrant after a four day treatment period. Nagata et. al and Yaguchi et. al in their studies noted that oral administration of 1,2-dilynoleoylsnglycero-3-phosphocholine (DLPhtCho) alone or in combination with 1-palmitoyl-2-oleoylsnglycero-3-phosphocholine (POPhtCho) predominantly blocked the scopolamine induced dementia, but these effects were less pronounced in normal animals (57, 58). Additionally, unlike the four-day treatment protocol employed in the present study, previous studies evaluating phospholipids followed longer durations of drug treatment, which may have contributed to the improved learning and memory observed with phospholipids (57, 59, 60). The dose and the duration of therapy appears to be important parameters in the pro-cognitive effects observed with phospholipids. Thus, in the present study, the improved learning and memory following CN treatment can be attributed purely to the intrinsic action of Centella extract, and the contribution of Phospholipon® 90H appears to be non-significant.

Conclusions

In the present study, an attempt was made to enhance the aqueous solubility of SCE via its complexation with phospholipids (preparation of naturosomes). A central composite design was used to optimize the formulation and process variables. The prepared CN were evaluated for physicochemical, functional, and pharmacological attributes. The FTIR, DSC, PXRD, photomicroscopy, and the SEM studies indicated the successful formation of vesicular drug-phospholipid complex. The apparent solubility, the *in-vitro* dissolution, and the *ex-vivo* permeability studies indicated a significant improvement in the aqueous solubility, the drug release, and the membrane permeation of the SCE from the CN, respectively. The preliminary *in-vivo* pharmacological evaluation revealed a significantly higher efficacy (likely due to improved bioavailability) of the prepared CN compared to the pure extract, and a comparable efficacy with the standard drug, piracetam (200 mg/kg). The exact mechanism of the improved efficacy of the prepared CN, as well as the contribution of individual triterpenes to the pharmacological activity will require further detailed investigation. Additional studies analyzing the pharmacokinetic parameters are required to substantiate the increased absorption, and the enhanced bioavailability hypothesis.

References

1. [WHO guidelines for governments and consumers regarding the use of alternative therapies]. Rev Panam Salud Publica. 2004;16(3):218-21.
2. Teng Z, Yuan C, Zhang F, Huan M, Cao W, Li K, et al. Intestinal absorption and first-pass metabolism of polyphenol compounds in rat and their transport dynamics in Caco-2 cells. PLoS One. 2012;7(1):e29647. doi: 10.1371/journal.pone.0029647.
3. Khan J, Alexander A, Ajazuddin, Saraf S, Saraf S. Recent advances and future prospects of phyto-phospholipid complexation technique for improving pharmacokinetic profile of plant actives. J Control Release. 2013;168(1):50-60. doi: 10.1016/j.jconrel.2013.02.025.
4. Husch J, Bohnet J, Fricker G, Skarke C, Artaria C, Appendino G, et al. Enhanced absorption of boswellic acids by a lecithin delivery form (Phytosome((R))) of Boswellia extract. Fitoterapia. 2013;84:89-98. doi: 10.1016/j.fitote.2012.10.002.
5. Freag MS, Elnaggar YS, Abdallah OY. Lyophilized phytosomal nanocarriers as platforms for enhanced diosmin delivery: optimization and ex vivo permeation. Int J Nanomedicine. 2013;8:2385-97. doi: 10.2147/ijn.s45231.
6. Kennedy DO, Haskell CF, Mauri PL, Scholey AB. Acute cognitive effects of standardised Ginkgo biloba extract complexed with phosphatidylserine. Hum Psychopharmacol. 2007;22(4):199-210. doi: 10.1002/hup.837.
7. Mukherjee K, Venkatesh M, Venkatesh P, Saha BP, Mukherjee PK. Effect of soy phosphatidyl choline on the bioavailability and nutritional health benefits of resveratrol. Food Research International. 2011;44(4):1088-93. doi: http://dx.doi.org/10.1016/j.foodres.2011.03.034.
8. Pathan R, Bhandari U. Preparation & characterization of embelin–phospholipid complex as effective drug delivery tool. J Incl Phenom Macrocycl Chem. 2011;69(1-2):139-47. doi: 10.1007/s10847-010-9824-2.
9. Zaidi SMA, Pathan SA, Ahmad FJ, Surender S, Jamil S, Khar RK. Neuropharmacological Evaluation of Paeonia emodi Root Extract Phospholipid Complex in Mice. Planta Med. 2011;77(05):P_123. doi: 10.1055/s-0031-1273652.
10. Huang Y, Mucke L. Alzheimer mechanisms and therapeutic strategies. Cell. 2012;148(6):1204-22. doi: 10.1016/j.cell.2012.02.040.
11. Association As. Alzheimer's Disease Facts and Figures. Alzeimer's & Dimentia. 2014;10(2).
12. Cappell J, Herrmann N, Cornish S, Lanctot KL. The pharmacoeconomics of cognitive enhancers in moderate to severe Alzheimer's disease. CNS Drugs. 2010;24(11):909-27. doi: 10.2165/11539530-000000000-00000.
13. Paris D, Mathura V, Ait-Ghezala G, Beaulieu-Abdelahad D, Patel N, Bachmeier C, et al. Flavonoids lower Alzheimer's Abeta production via an NFkappaB dependent mechanism. Bioinformation. 2011;6(6):229-36.
14. Jones WP, Chin YW, Kinghorn AD. The role of pharmacognosy in modern medicine and pharmacy. Curr Drug Targets. 2006;7(3):247-64.
15. Akhondzadeh S, Noroozian M, Mohammadi M, Ohadinia S, Jamshidi AH, Khani M. Salvia officinalis extract in the treatment of patients with mild to moderate Alzheimer's disease: a double blind, randomized and placebo-controlled trial. J Clin Pharm Ther. 2003;28(1):53-9.
16. Ha GT, Wong RK, Zhang Y. Huperzine a as potential treatment of Alzheimer's disease: an assessment on chemistry, pharmacology, and clinical studies. Chem Biodivers. 2011;8(7):1189-204. doi: 10.1002/cbdv.201000269.

17. Hossain S, Hashimoto M, Katakura M, Al Mamun A, Shido O. Medicinal value of asiaticoside for Alzheimer's disease as assessed using single-molecule-detection fluorescence correlation spectroscopy, laser-scanning microscopy, transmission electron microscopy, and in silico docking. BMC Complement Altern Med. 2015;15:118. doi: 10.1186/s12906-015-0620-9.
18. Lee TF, Shiao YJ, Chen CF, Wang LC. Effect of ginseng saponins on beta-amyloid-suppressed acetylcholine release from rat hippocampal slices. Planta Med. 2001;67(7):634-7. doi: 10.1055/s-2001-17366.
19. Zhang L, Qin C, Yuan S, Wang S. Application of Evodiamine in preparing medicaments for Alzheimer's disease. In: USPTO, editor. Google Patents. USA: Institute Of Laboratory Animal Science, Chinese Academy Of Medical Sciences; 2011.
20. Brinkhaus B, Lindner M, Schuppan D, Hahn EG. Chemical, pharmacological and clinical profile of the East Asian medical plant Centella asiatica. Phytomedicine. 2000;7(5):427-48.
21. Hashim P, Sidek H, Helan MH, Sabery A, Palanisamy UD, Ilham M. Triterpene composition and bioactivities of Centella asiatica. Molecules. 2011;16(2):1310-22. doi: 10.3390/molecules16021310.
22. Upadhyay SK, Saha A, Bhatia BD, Kulkarni KS. Evaluation of the efficacy of Mentat in children with learning disability: A placebo-controlled double-blind clinical trial. Neurosciences Today. 2002;VI(3):184-8.
23. Dave VS, Saoji SD, Raut NA, Haware RV. Excipient variability and its impact on dosage form functionality. J Pharm Sci. 2015;104(3):906-15. doi: 10.1002/jps.24299.
24. Bhattacharyya S, Majhi S, Saha BP, Mukherjee PK. Chlorogenic acid-phospholipid complex improve protection against UVA induced oxidative stress. J Photochem Photobiol B. 2014;130:293-8. doi: 10.1016/j.jphotobiol.2013.11.020.
25. Yue PF, Zhang WJ, Yuan HL, Yang M, Zhu WF, Cai PL, et al. Process optimization, characterization and pharmacokinetic evaluation in rats of ursodeoxycholic acid-phospholipid complex. AAPS PharmSciTech. 2008;9(1):322-9. doi: 10.1208/s12249-008-9040-1.
26. Yue P-F, Yuan H-L, Li X-Y, Yang M, Zhu W-F. Process optimization, characterization and evaluation in vivo of oxymatrine–phospholipid complex. International Journal of Pharmaceutics. 2010;387(1–2):139-46. doi: http://dx.doi.org/10.1016/j.ijpharm.2009.12.008.
27. Bhattacharyya S, Ahammed SM, Saha BP, Mukherjee PK. The gallic acid-phospholipid complex improved the antioxidant potential of gallic acid by enhancing its bioavailability. AAPS PharmSciTech. 2013;14(3):1025-33. doi: 10.1208/s12249-013-9991-8.
28. Tan Q, Liu S, Chen X, Wu M, Wang H, Yin H, et al. Design and evaluation of a novel evodiamine-phospholipid complex for improved oral bioavailability. AAPS PharmSciTech. 2012;13(2):534-47. doi: 10.1208/s12249-012-9772-9.
29. Bhattacharyya S, Ahmmed SM, Saha BP, Mukherjee PK. Soya phospholipid complex of mangiferin enhances its hepatoprotectivity by improving its bioavailability and pharmacokinetics. J Sci Food Agric. 2014;94(7):1380-8. doi: 10.1002/jsfa.6422.
30. Sze A, Erickson D, Ren L, Li D. Zeta-potential measurement using the Smoluchowski equation and the slope of the current-time relationship in electroosmotic flow. J Colloid Interface Sci. 2003;261(2):402-10. doi: 10.1016/s0021-9797(03)00142-5.
31. Saoji SD, Atram SC, Dhore PW, Deole PS, Raut NA, Dave VS. Influence of the Component Excipients on the Quality and Functionality of a Transdermal Film Formulation. AAPS PharmSciTech. 2015. doi: 10.1208/s12249-015-0322-0.
32. Singh D, Rawat MSM, Semalty A, Semalty M. Chrysophanol–phospholipid complex. J Therm Anal Calorim. 2013;111(3):2069-77. doi: 10.1007/s10973-012-2448-6.

33. Zhang Z, Chen Y, Deng J, Jia X, Zhou J, Lv H. Solid dispersion of berberine–phospholipid complex/TPGS 1000/SiO2: preparation, characterization and in vivo studies. International Journal of Pharmaceutics. 2014;465(1–2):306-16. doi: http://dx.doi.org/10.1016/j.ijpharm.2014.01.023.
34. Anderson NH, Bauer M, Boussac N, Khan-Malek R, Munden P, Sardaro M. An evaluation of fit factors and dissolution efficiency for the comparison of in vitro dissolution profiles. J Pharm Biomed Anal. 1998;17(4-5):811-22.
35. Dixit P, Jain DK, Dumbwani J. Standardization of an ex vivo method for determination of intestinal permeability of drugs using everted rat intestine apparatus. Journal of Pharmacological and Toxicological Methods. 2012;65(1):13-7. doi: http://dx.doi.org/10.1016/j.vascn.2011.11.001.
36. Vorhees CV, Williams MT. Morris water maze: procedures for assessing spatial and related forms of learning and memory. Nat Protoc. 2006;1(2):848-58. doi: 10.1038/nprot.2006.116.
37. Kumar A, Dogra S, Prakash A. Neuroprotective Effects of Centella asiatica against Intracerebroventricular Colchicine-Induced Cognitive Impairment and Oxidative Stress. Int J Alzheimers Dis. 2009. doi: 10.4061/2009/972178.
38. Veerendra Kumar MH, Gupta YK. Effect of different extracts of Centella asiatica on cognition and markers of oxidative stress in rats. J Ethnopharmacol. 2002;79(2):253-60.
39. Qin X, Yang Y, Fan TT, Gong T, Zhang XN, Huang Y. Preparation, characterization and in vivo evaluation of bergenin-phospholipid complex. Acta Pharmacol Sin. 2010;31(1):127-36. doi: 10.1038/aps.2009.171.
40. LeFevre ME, Olivo R, Vanderhoff JW, Joel DD. Accumulation of latex in Peyer's patches and its subsequent appearance in villi and mesenteric lymph nodes. Proc Soc Exp Biol Med. 1978;159(2):298-302.
41. Savic R, Luo L, Eisenberg A, Maysinger D. Micellar nanocontainers distribute to defined cytoplasmic organelles. Science. 2003;300(5619):615-8. doi: 10.1126/science.1078192.
42. Freitas C, Müller RH. Effect of light and temperature on zeta potential and physical stability in solid lipid nanoparticle (SLN™) dispersions. International Journal of Pharmaceutics. 1998;168(2):221-9. doi: http://dx.doi.org/10.1016/S0378-5173(98)00092-1.
43. Rarokar NR, Saoji SD, Raut NA, Taksande JB, Khedekar PB, Dave VS. Nanostructured Cubosomes in a Thermoresponsive Depot System: An Alternative Approach for the Controlled Delivery of Docetaxel. AAPS PharmSciTech. 2015. doi: 10.1208/s12249-015-0369-y.
44. Jena SK, Singh C, Dora CP, Suresh S. Development of tamoxifen-phospholipid complex: novel approach for improving solubility and bioavailability. Int J Pharm. 2014;473(1-2):1-9. doi: 10.1016/j.ijpharm.2014.06.056.
45. Maiti K, Mukherjee K, Gantait A, Saha BP, Mukherjee PK. Curcumin–phospholipid complex: Preparation, therapeutic evaluation and pharmacokinetic study in rats. International Journal of Pharmaceutics. 2007;330(1–2):155-63. doi: http://dx.doi.org/10.1016/j.ijpharm.2006.09.025.
46. Semalty A, Semalty M, Singh D, Rawat MSM. Phyto-phospholipid complex of catechin in value added herbal drug delivery. J Incl Phenom Macrocycl Chem. 2012;73(1-4):377-86. doi: 10.1007/s10847-011-0074-8.
47. Singh D, Rawat MSM, Semalty A, Semalty M. Emodin–phospholipid complex. J Therm Anal Calorim. 2012;108(1):289-98. doi: 10.1007/s10973-011-1759-3.

48. Singh C, Bhatt TD, Gill MS, Suresh S. Novel rifampicin-phospholipid complex for tubercular therapy: synthesis, physicochemical characterization and in-vivo evaluation. Int J Pharm. 2014;460(1-2):220-7. doi: 10.1016/j.ijpharm.2013.10.043.
49. Zhang K, Gu L, Chen J, Zhang Y, Jiang Y, Zhao L, et al. Preparation and evaluation of kaempferol–phospholipid complex for pharmacokinetics and bioavailability in SD rats. Journal of Pharmaceutical and Biomedical Analysis. 2015;114(0):168-75. doi: http://dx.doi.org/10.1016/j.jpba.2015.05.017.
50. Semalty A, Semalty M, Singh D, Rawat MSM. Preparation and characterization of phospholipid complexes of naringenin for effective drug delivery. J Incl Phenom Macrocycl Chem. 2010;67(3-4):253-60. doi: 10.1007/s10847-009-9705-8.
51. Xia HJ, Zhang ZH, Jin X, Hu Q, Chen XY, Jia XB. A novel drug-phospholipid complex enriched with micelles: preparation and evaluation in vitro and in vivo. Int J Nanomedicine. 2013;8:545-54. doi: 10.2147/ijn.s39526.
52. Mohandas Rao KG, Muddanna Rao S, Gurumadhva Rao S. Centella asiatica (L.) leaf extract treatment during the growth spurt period enhances hippocampal CA3 neuronal dendritic arborization in rats. Evidence-based complementary and alternative medicine : eCAM. 2006;3(3):349-57. doi: 10.1093/ecam/nel024.
53. Mohandas Rao KG, Muddanna Rao S, Gurumadhva Rao S. Enhancement of Amygdaloid Neuronal Dendritic Arborization by Fresh Leaf Juice of Centella asiatica (Linn) During Growth Spurt Period in Rats. Evidence-based complementary and alternative medicine : eCAM. 2009;6(2):203-10. doi: 10.1093/ecam/nem079.
54. Sikarwar MS, Sharma S, Jain AK, Parial SD. Preparation, Characterization and Evaluation of Marsupsin–Phospholipid Complex. AAPS PharmSciTech. 2008;9(1):129-37. doi: 10.1208/s12249-007-9020-x.
55. Yanyu X, Yunmei S, Zhipeng C, Qineng P. The preparation of silybin-phospholipid complex and the study on its pharmacokinetics in rats. Int J Pharm. 2006;307(1):77-82. doi: 10.1016/j.ijpharm.2005.10.001.
56. Ladd SL, Sommer SA, LaBerge S, Toscano W. Effect of phosphatidylcholine on explicit memory. Clinical neuropharmacology. 1993;16(6):540-9.
57. Nagata T, Yaguchi T, Nishizaki T. DL- and PO-phosphatidylcholines as a promising learning and memory enhancer. Lipids in health and disease. 2011;10:25. doi: 10.1186/1476-511x-10-25.
58. Yaguchi T, Nagata T, Nishizaki T. Dilinoleoylphosphatidylcholine ameliorates scopolamine-induced impairment of spatial learning and memory by targeting α7 nicotinic ACh receptors. Life Sciences. 2009;84(9–10):263-6. doi: http://dx.doi.org/10.1016/j.lfs.2008.12.003.
59. Yaguchi T, Nagata T, Nishizaki T. 1-Palmitoyl-2-oleoyl-sn-glycero-3-phosphocholine improves cognitive decline by enhancing long-term depression. Behavioural brain research. 2009;204(1):129-32. doi: 10.1016/j.bbr.2009.05.027.
60. Chung SY, Moriyama T, Uezu E, Uezu K, Hirata R, Yohena N, et al. Administration of phosphatidylcholine increases brain acetylcholine concentration and improves memory in mice with dementia. The Journal of nutrition. 1995;125(6):1484-9.

Response to reviewer's comments

Reviewers' Comments:

Editorial office note:

1. ALL experimental and estimated values should be reported to 3 significant figures only, unless justification is explicitly stated to document a higher degree of accuracy. Errors should not be provided with a higher degree of accuracy than the mean value, for example 20.2 +/- 3.55 should be written as 20.2 +/- 3.6.

RESPONSE: Suggestions have been incorporated in the revised manuscript.

2. Please reduce the total number of figures + tables to no more than 10, in compliance with the INSTRUCTIONS TO AUTHORS. Some of the less important figures and tables can be moved to be SUPPLEMENTARY MATERIALS, which will be linked to the article, and accessible to readers. Please adjust the text accordingly in reference to the altered numbering of the figures and tables.

RESPONSE: We have reduced the number of figures to 7 and the number of tables to 3, in compliance with the total number not to exceed 10.

Editor's comments:

Please address the reviewer's comments, and also please add a scale bar to Figure 3.

RESPONSE: A scale bar is now added to the figure. The figure is now moved to be supplementary materials (Suppl. Figure 2).

Reviewer #1:

1. Nicely written article.

RESPONSE: Thank you, the authors appreciate the encouragement.

2. Reviewer will highly encourage to add more discussion for pharmacological evaluations.

RESPONSE: The pharmacological evaluations are further elaborated in the manuscript.

3. Reviewer will recommend adding a separate section correlating the solubility/ dissolution/ release studies with animal studies presented in the manuscript.

RESPONSE: Additional discussion correlating the solubility/dissolution with animal studies added to the manuscript.

Reviewer #2:

The authors describe the generation of a phospholipid-Standardized Centella Extract (SCE) complex for the treatment of Alzheimer's disease. It was proposed that complexing this phytoconstituent with phospholipids would allow for an increase in aqueous solubility, dissolution rate, and permeation rate compared to pure SCE. A quality by design approach was employed to optimize the encapsulation efficiency of the SCE. In-vitro dissolution studies and ex-vivo permeation studies were performed to characterize the physiochemical properties of the complex. An in-vivo pharmacological study was performed to test the efficiency of the complex.

1. Figure 11: It seems that the mice treated with SCE and CN perform very similarly in experiment A and B. The significance in difference is very minimal and seems to be overstated by the authors. Moreover, a difference in Figure 11B of 2-3 seconds of time spent in target quadrant is most likely not biologically relevant. The authors should rephrase their discussion and their conclusion.

RESPONSE: The reviewer's comments are duly noted, and the discussion is appropriately rephrased.

<u>A brief explanation:</u>

The effect of SCE and CN on learning and memory was assessed in the aged mice (figure 7A and B). We noted that piracetam, ($p < 0.001$ on day 3 and 4), SCE ($p < 0.05$ day 3 and $p < 0.01$ on day 4), PM ($p < 0.05$ day 3 and $p < 0.01$ on day 4) and CN ($p < 0.05$ on day 2 and $p < 0.001$ on day 3 and 4) significantly decreased the escape latency, indicating improved learning and memory in aged mice. While these results emphasize the effectiveness of SCE in age related dementia, CN showed greater efficacy as compared to SCE. The escape latencies for both the treatment groups were as follows:

Days	Aged mice+SCE (sec)	Aged mice+CN (sec)	Difference (sec)
1	115.1	107.3	-7.810
2	89.64	77.31	-12.33
3	73.81	58.64	-15.17
4	55.37	25.82	-29.55

Statistical analysis (Bonferroni multiple comparison post hoc tests) of this data noted that, 4 day treatment of CN significantly decreased the escape latencies in aged mice as compared to SCE ($p<0.05$), indicating the superiority of CN over SCE. These effects may be attributed to the improved solubility and thus bioavailability in *in-vivo* studies. Although CN treated animals spent higher time in searching platform in the target

quadrant as compared with SCE treated animals, the observed difference was not statistically significant. The reason behind this observation is not well understood, but we may speculate that a continuous four-day treatment of *centella extract* through both the formulations produced long term effects on memory in the aged animals, and thus significantly increased time spent in the target quadrant. Interestingly, a significant time spent in the target quadrant was exhibited only in CN treated animals ($p<0.05$) but not in SCE ($p<0.05$) treated group as compared to vehicle treated aged mice. These observations enabled us to conclude that the formulated CN exhibits improved bioavailability and efficacy in the treatment of Alzheimer's disease.

2. Pharmacological evaluation of the formulations: First, the authors should treat the mice with the Phospholipon 90H alone as a control. This is relevant because there is some evidence that lipids alone could reduce cognitive decline. For example, the Phospholipid Intervention for Cognitive Ageing Reversal investigates if phospholipids demonstrate cognitive benefits and memory retention benefits. Second, the authors should treat the mice with a control of the physical mixture of SCE and phospholipid. These controls were performed during the in-vitro and ex-vivo studies and the reviewer believes they should be included in the in-vivo study as well. Reference: Scholey, A.B., et al., A randomized controlled trial investigating the neurocognitive effects of Lacprodan(R) PL-20, a phospholipid-rich milk protein concentrate, in elderly participants with age-associated memory impairment: the Phospholipid Intervention for Cognitive Ageing Reversal (PLICAR): study protocol for a randomized controlled trial. Trials, 2013. 14: p. 404.

RESPONSE: The authors understand the reviewer's concern about *per se* effect of Phospholipon 90H on learning and memory. Therefore, we administered 900 mg/kg of Phospholipon 90H alone orally, and 1-hr thereafter the animals were subjected to MWM test. We did not observe any significant improvement in the escape latency or the time spent in the target quadrant, suggesting no effect of four-day treatment of Phospholipon 90H on learning and memory. The administration of the physical mixture of Phospholipon 90H-SCE to the aged mice exhibited similar escape latency as that of SCE treated animals.

Additional discussion is incorporated in the manuscript.

3. The authors claim in the first sentence of the abstract that the goal of the work was to improve the bioavailability of the phytoconstituent. Although, higher solubility was observed in vitro, this did not translate in better efficacy under in vivo conditions (SCE compared to CN. The authors should discuss why the higher solubility did not translate to better pharmacological effects/or why higher solubility does not necessarily mean better bioavailability (depends on the properties of the drugs).

RESPONSE: discussion is incorporated in the manuscript.

4. The authors used dynamic light scattering (DLS) and scanning electron microscopy (SEM) as techniques to quantify the size of the CN. There is a discrepancy between the size of the particle suggested by DLS, ~450 nm, and the size of the particles calculated by the reviewer using the scale bars included in Figure 4 (around 18 μm for Figure 4C). DLS may be an inappropriate technique to use because irregular shaped particles, such as the CN, will scatter light depending largely on the orientation of the particle in solution. If the SEM images are to be trusted, than the author's argument regarding the ability of smaller particles (<500 nm) to cross epithelial cell membranes via endocytosis is invalid for their proposed technology.

RESPONSE: The authors acknowledge reviewer's observations. The SEM and photomicroscopy techniques were used mainly to understand the surface morphology of the prepared CN, rather than particle size. Multiple replicates of CN samples evaluated with DLS showed a mean particle size of 450.1 ± 20.0 nm. While imaging may give some approximation of the size, considering the heterogeneity in the nature of the prepared particles, limited field of view, and the operator bias, the authors believe that SEM may not provide an accurate estimate of the particle size.

Minor point:

1. The authors abbreviated CN (Centella Naturosome) in the abstract and did not include an explanation. The explanation was however later clarified in the **introduction.**

RESPONSE: Comment noted. Changes are made to the abstract to reflect the explanation of the abbreviation.

Table 1: Coded levels and “Real” values for each factor under study

Table 2: Central composite design formulation batches with respective entrapment efficiencies. * Values represent mean ± standard deviation (n=3)

Table 3: Solubility study of SCE, PM and CN. *Data expressed as mean ± Std. Dev.; n = 3

Table

Table 1: Coded levels and "Real" values for each factor under study

Variables	Levels				
	-1.7	-1	0	+1	+1.7
Independent	**Real values**				
Phospholipid : drug ratio (X_1, w:w)	0.5	1.0	1.8	2.5	3.0
Reaction temperature (X_2, °C)	40.0	44.0	50.0	56.0	60.0
Reaction time (X_3, h)	1.0	1.4	2.0	2.6	3.0
Dependent					
Entrapment efficiency (Y, % w/w)					

Table 2: Central composite design formulation batches with respective entrapment efficiencies.

Batches	X_1	X_2	X_3	Entrapment efficiency* (%, w/w)
F1	-1	+1	+1	83.2 ± 1.3
F2	-1	-1	+1	89.2 ± 0.8
F3	+1.7	0	0	95.1 ± 1.1
F4	+1	-1	+1	86.4 ± 1.3
F5	0	0	-1.7	76.7 ± 0.9
F6	-1.7	0	0	58.1 ± 1.1
F7	0	0	+1.7	94.4 ± 1.2
F8	+1	+1	+1	94.3 ± 1.0
F9	0	-1.7	0	79.4 ± 0.9
F10	-1	-1	-1	64.7 ± 0.9
F11	-1	+1	-1	71.5 ± 0.8
F12	0	+1.7	0	90.9 ± 1.3
F13	+1	+1	-1	90.0 ± 1.1
F14	+1	-1	-1	82.2 ± 1.6
F15- F20	0	0	0	91.4 ± 0.9

* Values represent mean ± standard deviation (n=3)

Table 3: Solubility study of SCE, PM and CN.

Sample	Aqueous solubility (µg/ml)*	n-Octanol solubility (µg/ml)*
SCE	8.12 ± 0.44	325.33 ± 6.71
PM	13.58 ± 0.35	331.08 ± 5.89
CN	98.01 ± 1.37	343.16 ± 7.21

*Data expressed as mean ± Std. Dev.; n = 3

Fig. 1. Pareto diagrams for effect estimation. The effects presenting probability values higher than 0.05 are not considered as statistically significant

Fig. 2. FTIR spectra of (A) SCE, (B) phospholipid, (C) physical mixture, (D) CN.

Fig. 3. DSC thermograms of (A) SCE, (B) phospholipid, (C) physical mixture, (D) CN.

Fig. 4. PXRD spectra of (A) SCE, (B) phospholipid, (C) physical mixture, (D) CN.

Fig. 5. *In vitro* dissolution study of SCE, PM and CN

Fig. 6. *Ex Vivo* permeability study of SCE, PM and CN

Fig. 7. Effect of Standardized Centella Extract (SCE) and Centella Naturosomes (CN) on spatial learning and memory in the Morris Water Maze (MWM) test. (A) Young and aged animals were treated with vehicle (saline), Phospholipon® 90H (900 mg/kg), piracetam (200 mg/kg), SCE (300 mg/kg), physical mixture (equivalent to 300 mg/kg SCE), or CN (equivalent to 300 mg/kg SCE) via oral route, and 1 hour later subjected to assessment of escape latency in a four-day acquisition trial in MWM test. Data are expressed as mean ± SEM. $^{*}p < 0.01$, $^{**}p < 0.001$ vs young mice + vehicle; $^{\#}p < 0.05$, $^{\#\#}p < 0.01$, $^{\#\#\#}p < 0.001$ vs aged mice + vehicle. (B) Total time spent by the animals in the target quadrant during the probe trial on day 5. Data are expressed as mean ± SEM. $^{*}p < 0.05$ vs young mice + vehicle; $^{\#}p < 0.05$, $^{\#\#}p < 0.01$ vs aged mice + vehicle.

Figure 1

Click here to download Figure Figure 1 - Pareto.tiff

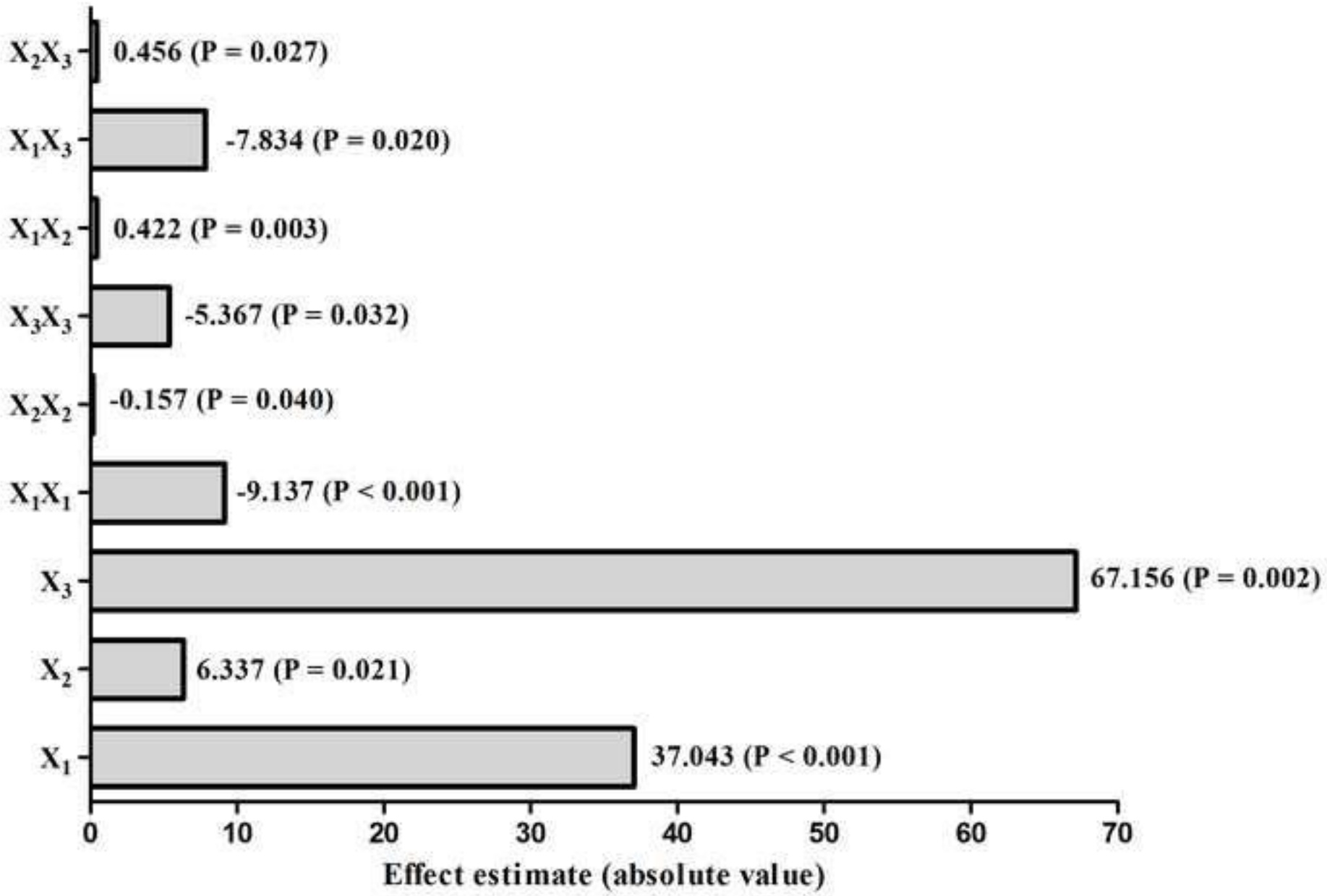

Figure 2

Click here to download Figure Figure 2 - FTIR.tiff

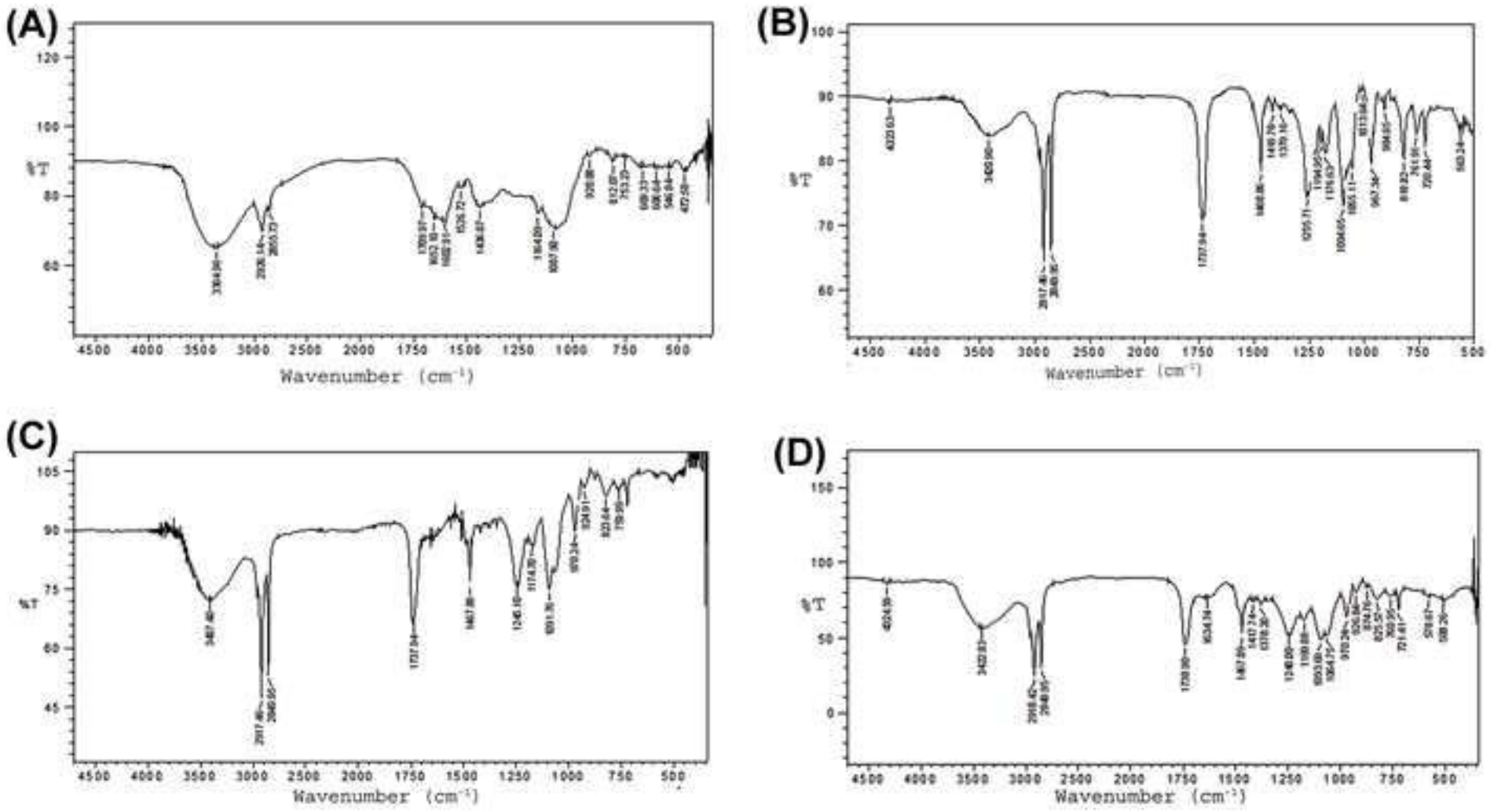

Figure 3

Click here to download Figure Figure 3 - DSC.tiff

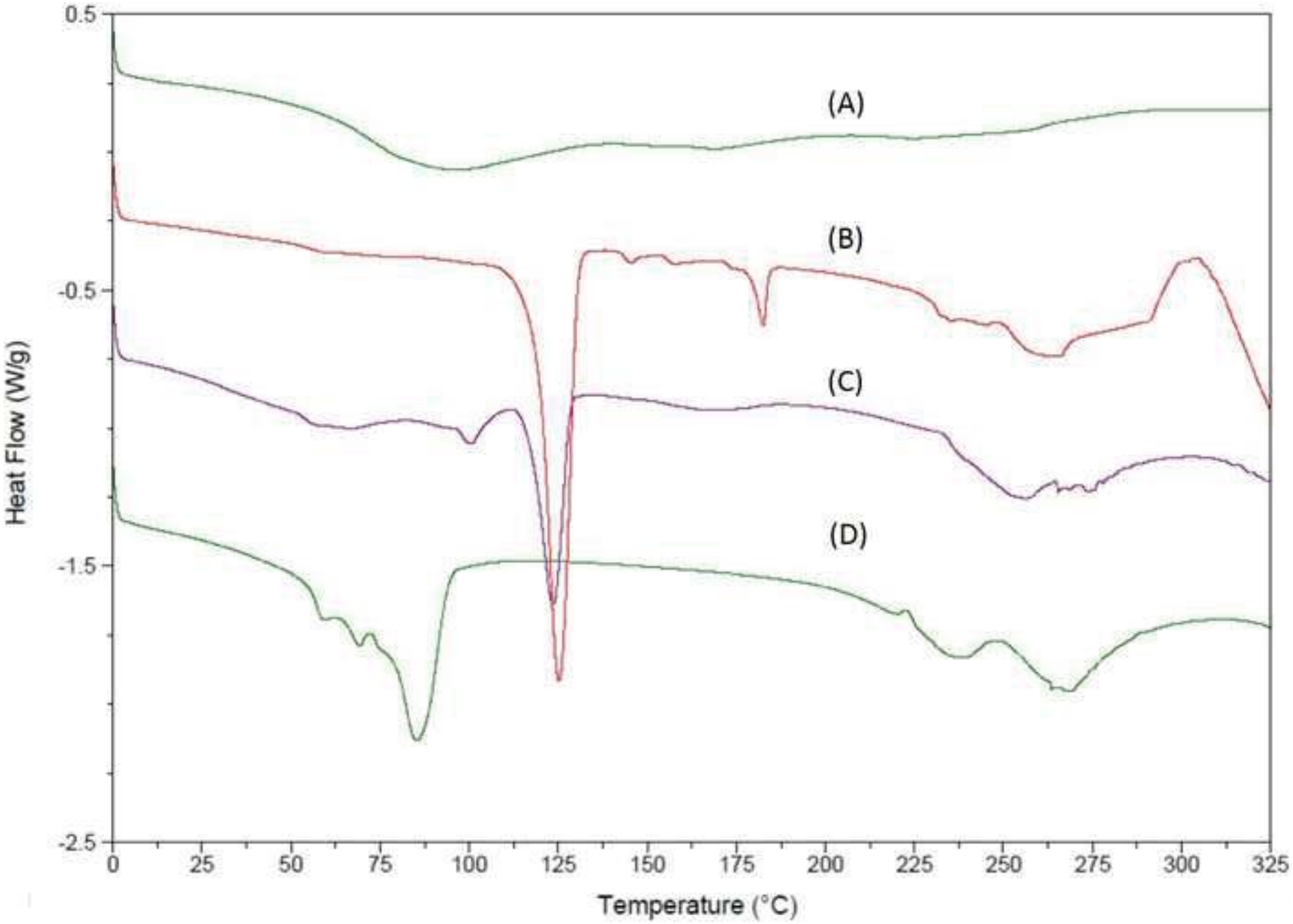

Figure 4

Click here to download Figure Figure 4 - Powder X-ray diffraction.tiff

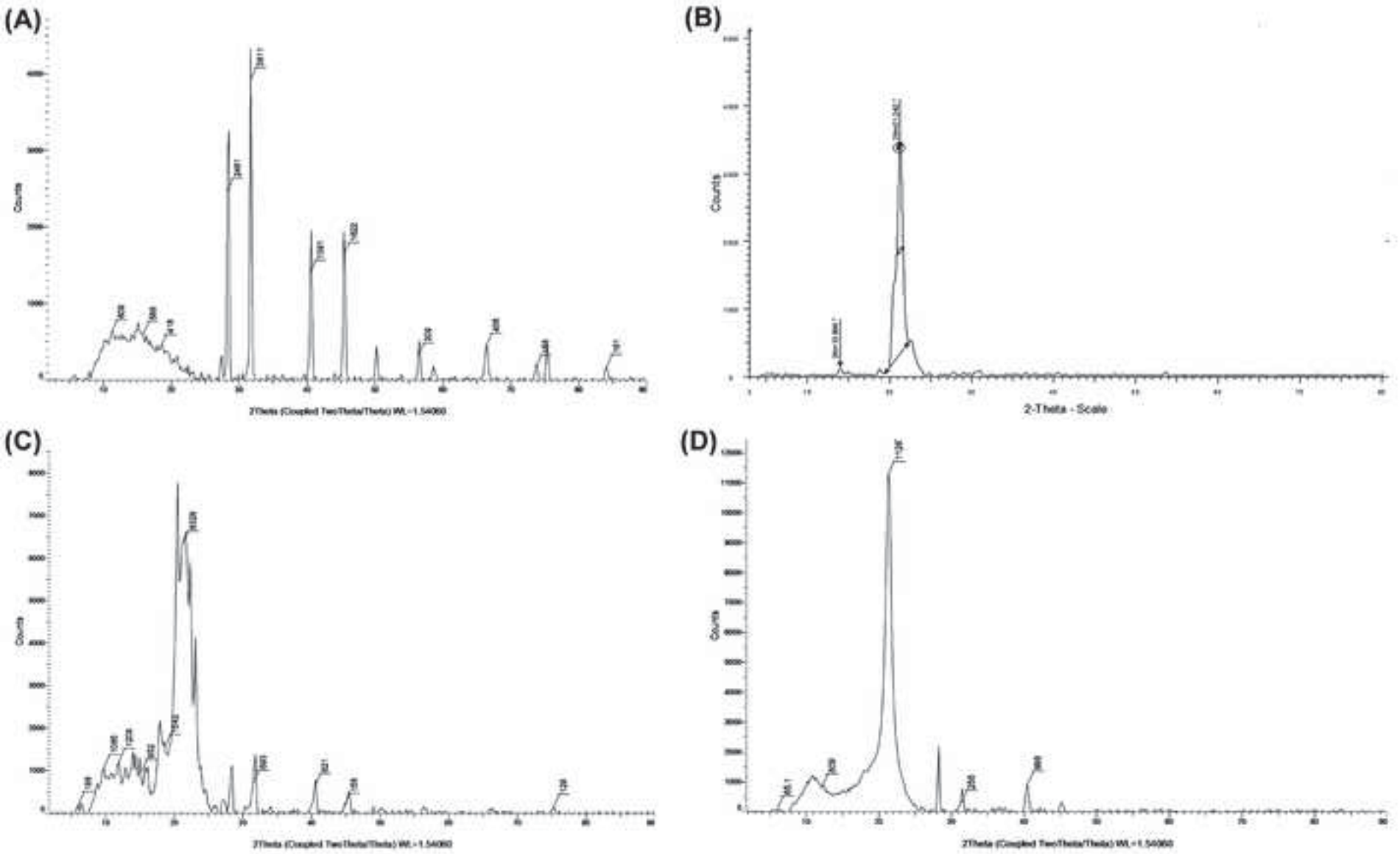

Figure 5

Click here to download Figure Figure 5 - In-vitro drug release.tiff

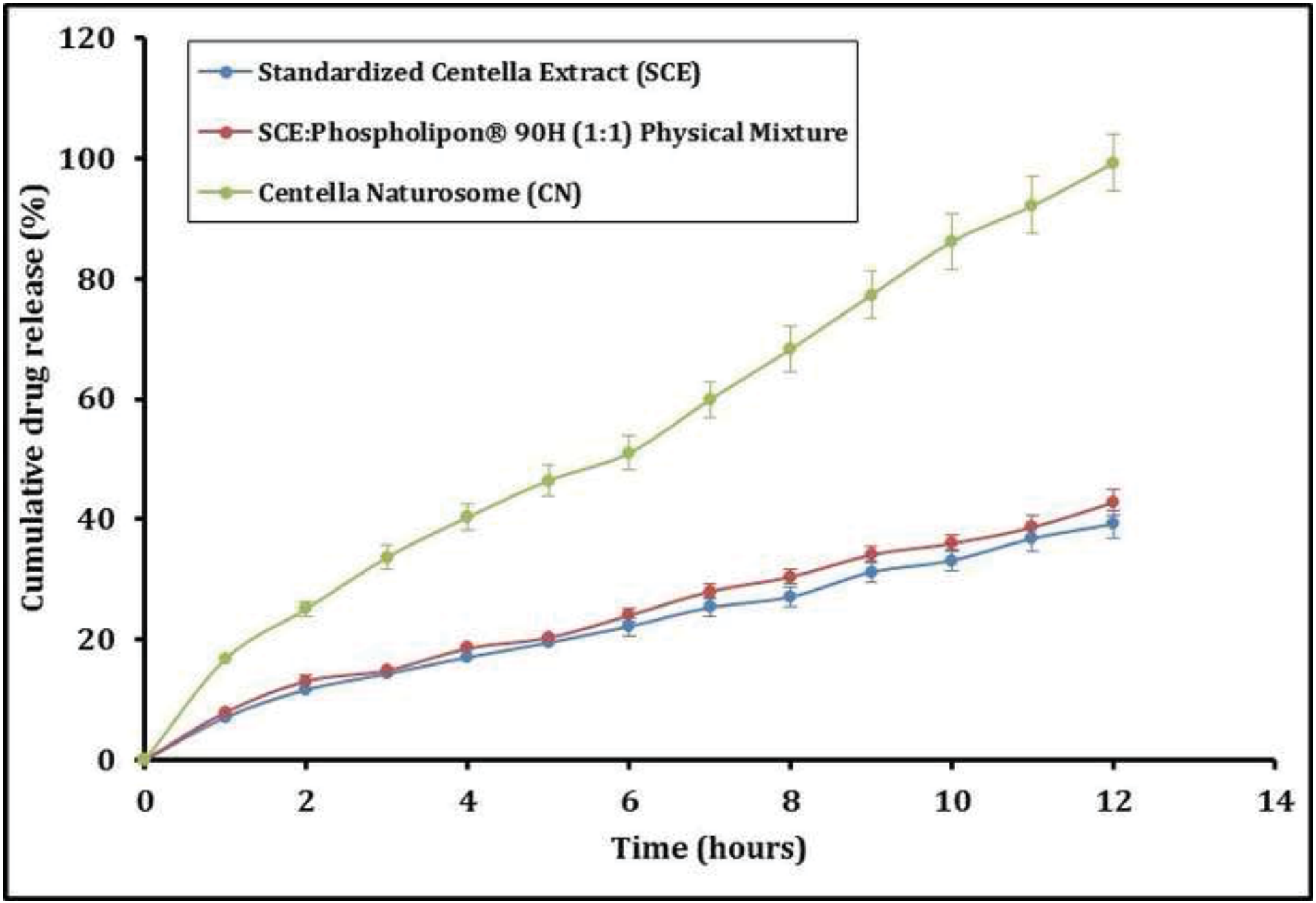

Figure 6

Click here to download Figure Figure 6 - Ex-vivo permeation.tiff

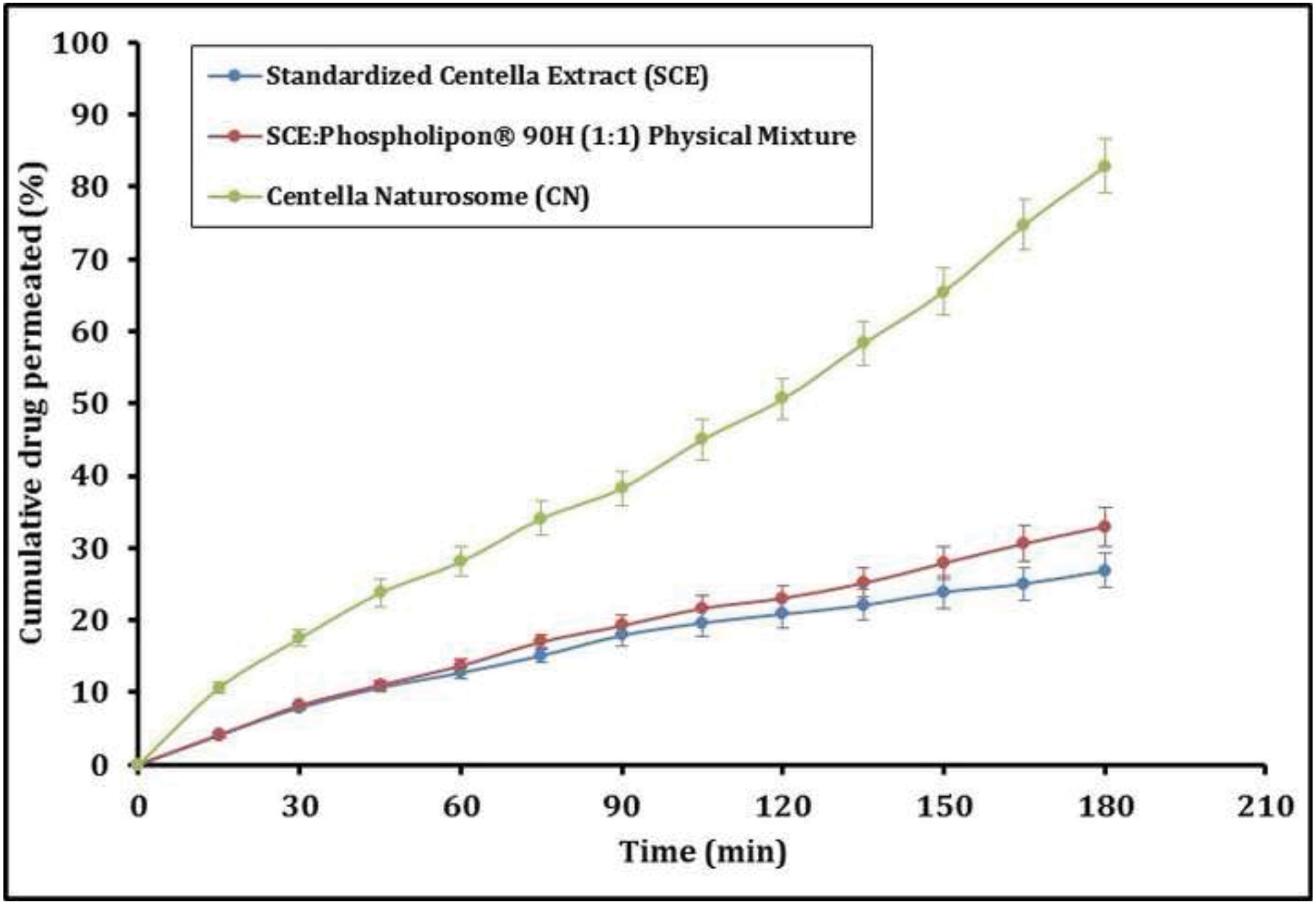

Figure 7

Click here to download Figure Figure 7 - In-vivo studies.tif